Three-dimensional numerical simulation of the temperature, potential and concentration distributions of a unit cell for various geometries of SOFC's

Raphaèle Herbin, Jean-Michel Fiard
Université de Savoie, France
James R. Ferguson
Baden, Switzerland.

1 Introduction

The work presented here deals with the mathematical modelling and numerical simulation of natural gas-fed solid oxide cells (Solid Oxide Fuel Cell, SOFC). The physics of fuel cell operation and the simplifying assumptions which are taken into account in the mathematical model are briefly presented in section 2. For a description of the principle of a SOFC, we refer to e.g [2], [6]. A selection of the numerical results obtained with the mathematical model are presented here. First a comparison with a benchmark which was performed by participants of the IEA project on SOFC's [1], was made in order to validate the numerical code; then some results showing efficiencies of the different planar geometries are presented. The adaptivity of the numerical code allows the simulation of cylindrical and tubular geometries. Some results are shown in section 4. Finally, numerical results with a more elaborate model including internal reforming are given in section 5.

2 Numerical model of a cell

2.1 The mathematical model

A 3D model of a cell is obtained by writing the conservation laws in the solid parts of the cell for heat, electrical current and mass (the latter in the porous parts only), and the conservation of heat and mass in the air and fuel channels. We consider here steady state operation, hence the phenomena are not time-dependent. The unknowns of the mathematical model are the temperature T at any point of the solid or the

channels, the electrical potential Φ at any point of the solid part of the SOFC, and the molar fractions X_i of the various species ($i = O_2, H_2, H_2O, CO, CO_2, CH_4$) at any point of the channels and in the porous media of the solid part of the cell. The heat flux is written with respect to the temperature using Fourier's law of heat conduction; the electrical current is written w.r.t. the electrical potential using Ohm's law, and the mass flux is written using Fick's law of diffusion (see [3] for details). A volumetric heat source term is introduced to account for the ohmic heat generation. A heat surface source term is introduced at the anode/electrolyte interface, due to the exothermic electrochemical reaction. Finally, the electrochemical potential jump between anode and cathode is modelled by Nernst's law. In section 3.1, the overpotentials at the cathode and the anode are set equal to the ohmic loss of the electrolyte, whereas we used the expressions given by [13] for the other computations. The resulting set of equations is a system of coupled nonlinear elliptic equations, the detail of which may be found in e.g. [9].

2.2 The numerical procedure

The necessary step in order to perform a numerical simulation is to discretize the set of equations in T, Φ and X_i. The equations themselves are of the Laplace type in the solid part and can be successfully discretized by any of the usual methods, i.e. finite differences, finite element or finite volumes. However finite volume discretization (see [12], [10] for an introduction) was preferred over the finite element method because it is computationally cheaper, as can be seen in the results shown in [9]. Moreover, an advantage of the finite volume method is that it is "close to the physics" in the sense that it is based on writing the balance of the fluxes through the boundaries of a discretization cell (which is called a "control volume"), and therefore all source terms can be accounted for in a natural way. The discretization of the equations yields a nonlinear finite system, where the unknowns are the average values (over the control volumes) of T, Φ and X_i. The equations in T, Φ, X_i are coupled by the electrical conductivity (which depends on the temperature), the ohmic source terms and the interface source terms, both in T and Φ. A rather straightforward iterative method is used, which computes, for a given temperature, the solution to the mass and electric problems (X_i and Φ), and once convergence is obtained, solves the temperature problem.

2.3 Description of the computer program

The computer program consists of two parts. The first part is the computational kernel and database manager. It was written using the C language and contains 11000 lines. It has been used on several UNIX systems: Silicon Graphics, SUN, CRAY. The database input file contains the parameters which define the geometries (planar, cylindrical or tubular), the composition of the fuel (hydrogen or methane),

the computational mesh and the set of operating conditions. (Currently, a user-friendly graphic X interface is being developped.) The second part is a 10000 lines graphic software which includes a user-friendly mesh generator and a 3D-graphics post-processor. This part uses some efficient Silicon Graphics libraries such as GL, ImgTools or FontManager which can be used only on Silicon Graphics systems. The results which are presented here were obtained on a INDIGO SG worksation with a 50MHz R4000 processor and 32 MB of real memory. The database file requires about 100 MB of disk memory.

2.4 General operating conditions

The next three sections are devoted to the numerical results which were obtained by running the code on different geometries of adiabatic cells. The code can simulate a cell using pure hydrogen only, or using methane with internal reforming. Tables 1 and 2 gives the operating parameters for both cases. The mean electrical current density, which is also an input parameter, is ommitted here because it depends on the run. The general operating conditions were taken as in [1], whereas the operating conditions concerning internal reforming were taken from [13].

Gas	Temp.	O_2	N_2	H_2	H_2O	CO	CO_2	CH_4
Air	1173 K	21 %	79 %					
Fuel I	1173 K			90 %	10 %			
Fuel II	1173 K			26.26 %	49.34 %	2.94 %	4.36 %	17.10 %

Table 1: Gas temperature and composition at inlet

Fuel utilization	85 %			
Air ratio	7			
Pressure	1 bar			
Electrical σ $(\Omega^{-1}m^{-1})$ and thermal λ $(Wm^{-1}K^{-1})$ conductivities				
	Cathode	Electrolyte	Anode	Interconnect
σ	$\frac{4.2\,10^7}{T}exp-\frac{1200}{T}$	$3.34\,10^4 exp-\frac{10300}{T}$	$\frac{9.5\,10^7}{T}exp-\frac{1150}{T}$	$\frac{9.3\,10^6}{T}exp-\frac{1100}{T}$
λ	2	2	2	2
Diffusion coefficient	D_{O_2}	D_{H_2}	D_i (Fuel II)	
Values (cm^2s^{-1})	$0.181 * \left(\frac{T}{273}\right)^{1.5}$	$0.753 * \left(\frac{T}{273}\right)^{1.5}$	$0.364 * \left(\frac{T}{273}\right)^{1.5}$	

Table 2: General operating conditions

3 The hydrogen model for planar geometries

Numerical runs involving the hydrogen model on planar geometries will be presented here. In order to validate our code, we compare the results given by our code on a benchmark which was defined by participants of the IEA program for the numerical simulation of a planar geometry with 18 fuel and air channels. We then compare the efficiencies of the three geometries.

3.1 Comparison with the IEA benchmark

Numerical tests were performed in the case of the co- and counter-flow for a planar geometry of one rectangular channels with the following parameters: active area 5.42x100 mm^2, anode thickness 50 μm, cathode thickness 50 μm, electrolyte thickness 150 μm, channel width 3mm, channel height 1mm, rib width 2.42 mm, total bipolar plate thickness 2.5 mm, and for a mean current density of $300 mA/cm^2$. We found

	Cell voltage		*Max solid temp*		*Min solid temp*	
Author	counter	co	counter	co	counter	co
Dornier (D)	0.689	0.684	1085	1070	914	928
ECN Petten (NL)	—	0.704	—	1082	—	899
Eniricerche (I)	0.730	0.722	1083	1069	906	916
Inst. for energiteknikk (N)	0.71	0.71	1084	1058	912	930
KFA-Jülich (D)	0.712	0.706	1073	1059	906	913
Siemens (D)	0.716	0.712	1062	1049	904	909
Statoil (N)	0.709	0.702	1082	1098	913	970
Risø (DK)	0.7101	0.7034	1075	1061	910	924
GDF Univ. Savoie (2D diff.)	0.7080	0.6955	1055	1037	920	921
GDF Univ. Savoie (1D diff.)	0.7203	0.7079	1054	1036	920	918

Table 3: Comparison with the IEA benchmark

that the cell voltage which we obtained with our inital model (labeled "2D diff") could be significantly increased if the diffusion of the gas in the porous medium was taken to be only in the direction normal to the electrolyte/anode interface (which is the case in most models and in our simplified model labeled "1D diff"). In our model, however, the diffusion effect is accounted for in all directions, and the hydrogen concentration at the electrode/electrolyte interface is much lower away from the channel than close to it. These results show the advantage of wide channels and narrow ribs.

3.2 Comparison of the co-, counter- and cross- flow cases

Figure 1 gives a comparison of the efficiency (i.e. the ratio of electrical energy to chemical energy at inlet) of geometry with 5 fuel and air channels for the co-, counter- and cross- flow designs, as a function of current density.
These computations show the counter flow design as being most efficient.

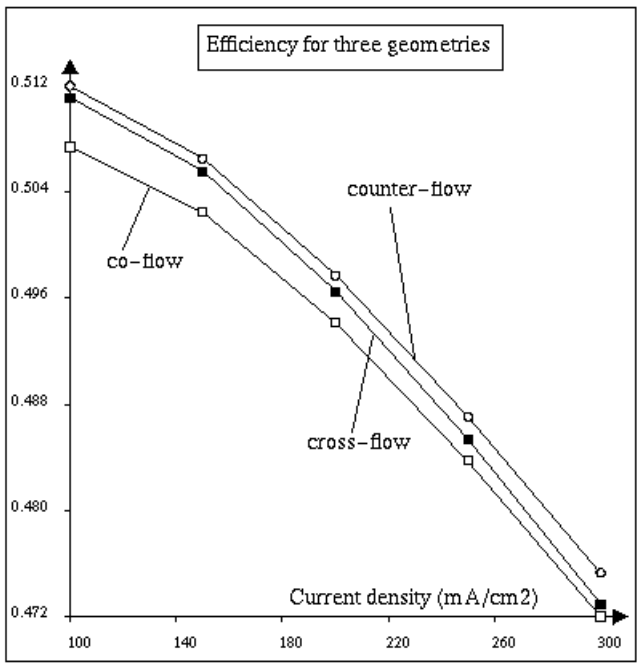

Figure 1: Efficiency of co-, counter- and cross- flow geometries

4 Results for other types of geometries

The adaptivity of our 3D SOFC code can be demonstrated by running numerical simulations on other fundamental geometries. Here a sample of results concerning a tubular (Westinghouse concept) geometry and a cylindrical geometry are given.

4.1 The tubular geometry

In this test, the mean current density is taken equal to 1500 mA/cm^2 in the interconnect. The dimensions of the cell were taken from [5] and [7] and are shown in Figures 2. Figure 2 also shows the contours of current density at the outlet section of the cell. It can be noted that the highest density is near the interconnect/anode interface; this is due to the fact that the anode is thin, and that the interconnect

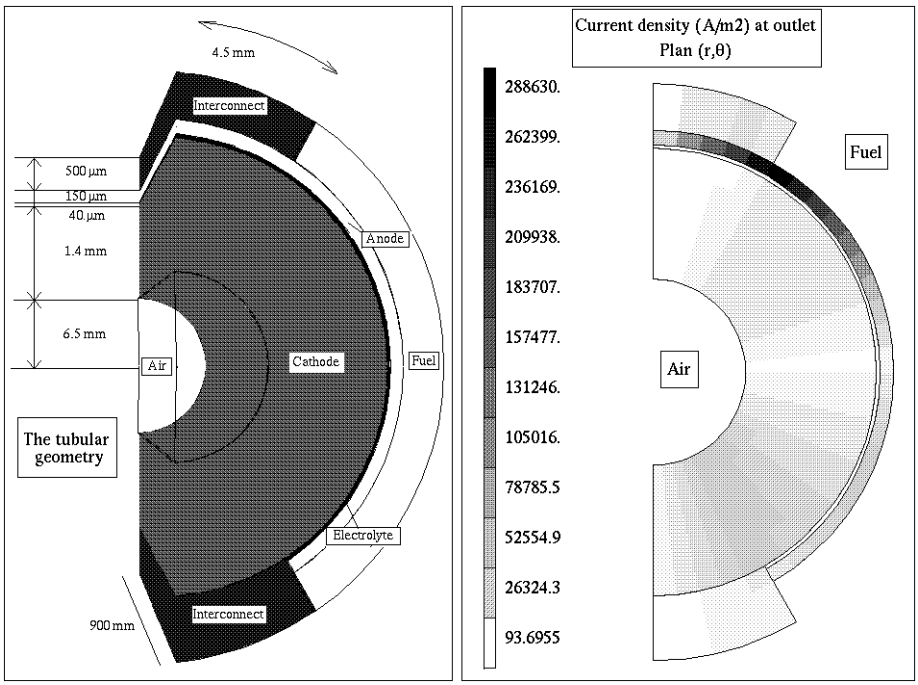

Figure 2: 3D section of the tubular design and current density at outlet section

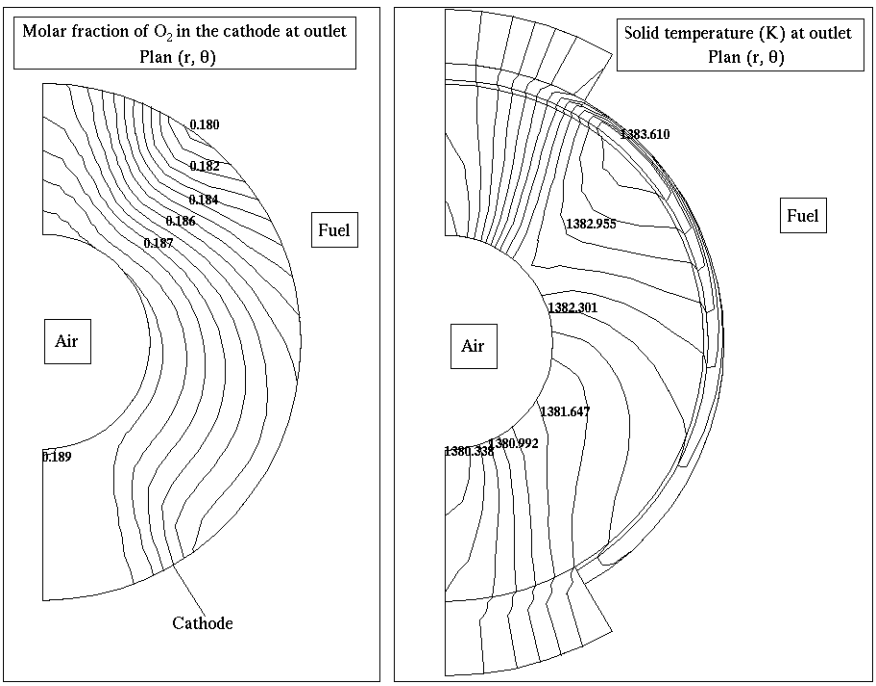

Figure 3: Molar fraction of O_2 and temperature at outlet section

area is not very large. On the cathode side, however, the current density is lower because the cathode is thicker. Figure 3 shows the contours of the molar fraction of oxygen and the temperature at the oulet section of the cells. Note that the minimum of the molar fraction of O_2 and the maximum temperature are reached in the region of highest current density.

4.2 The cylindrical geometry

In the absence of data for a so-called "cylindrical" geometry, we derived the dimensions of a cylindrical cell by distorting a planar cell. The dimensions of the cell are shown on Figure 4. The computations were performed on a "slice" of the cell only, taking symmetry considerations into account. the mean current density is taken equal to 180 mA/cm^2. Figure 5 shows the diffusion of hydrogen in the anode. Again, one can see that the diffusion is always weaker at the center of the rib.

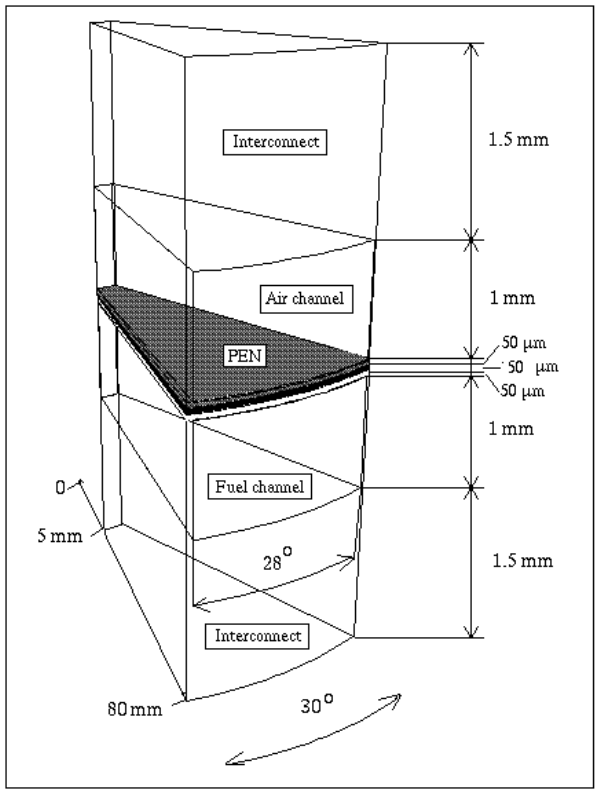

Figure 4: Geometry of a cylindrical cell

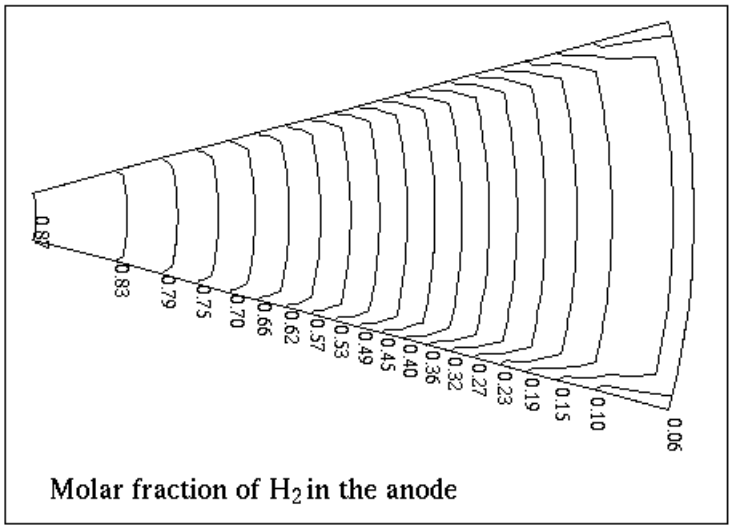

Figure 5: Molar fraction of H_2 in the anode

5 Some results on reforming

A model including internal reforming was established, using Fick's law of diffusion for CH_4, CO, CO_2, H_2 and H_2O in the porous media. The shift reaction is assumed to be at equilibrium, and the reforming reaction is taken into account by a methane degradation rate taken from the work of Lee [11]. The mean current density is taken equal to 160 mA/cm^2. Figure 6 shows the concentrations of methane, hydrogen and water in the fuel channel on the geometry used on the IEA benchmark. The CH_4 and H_2 molar fractions decrease while the H_20 molar fraction increases along the channel. Note also the 2D behaviour of the molar fractions: X_{H_2} and X_{CH_4} are lower away from the channel than close to it.
Cell performance using pure hydrogen (fuel I in table 1) and a mixture of methane and hydrogen (fuel II in table 1) can be compared. The efficiencies obtained with Fuel I and Fuel II are respectively 51.26 % and 51.87 %. Therefore internal reforming seems to be quite efficient.

6 Conclusion

A 3D numerical code was developped for the numerical simulation of solid oxide fuel cells and stacks. Due to space limitations, the results shown here only give a glimpse of the several numerical studies which may be achieved with the 3D code. In particular, one could perform sensitivity analysis for any of the geometries, with respect the geometry parameters, or w.r.t. the physical properties of the constitutive

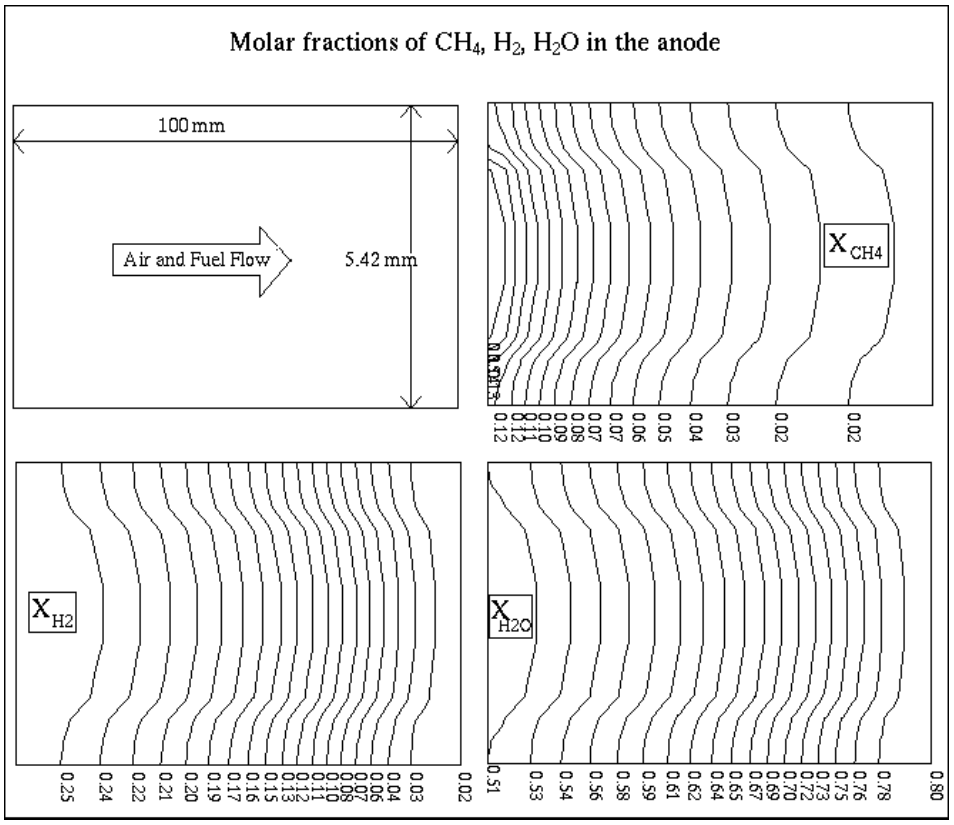

Figure 6: Molar fractions in the anode

materials or w.r.t. operating conditions.

Aknowledgement: The work of the second author was supported by Gaz de France and ADEME (Agence de l'Environnement et de la Maîtrise de l'Energie)

References

[1] E. Achenbach, Status of the IEA-Bench Mark Test 1 on stack modelling, *IEA workshop, Rome, February 22-25, 1994.*

[2] A.J. Appleby and F.R. Foulkes, Fuel Cell Handbook, *Van Nostrand Reinhold, New York, 1989.*

[3] R.B. Byrd, W.E. Stewart and E.N. Lightfoot , Transport Phenomena, *John Wiley and sons, 1960.*

[4] U.G. Bossel and J.R. Ferguson, Natural Gas Fuelled Solid Oxide Fuel Cells and Sytems, Facts and Figures, *International Energy Agency, workshop, Charmey, Switzerland, July 2-6, 1989.*

[5] R. Draper et al., Solid oxide fuel cell generator, *United States Patent 5,200,279, Apr. 6, 1993.*

[6] J.R. Ferguson, Analysis of Temperature and Current Distributions in Planar SOFC Designs, *2nd International Symposium on Solid Oxide Fuel Cells, July 2-5,1991, Athens, Greece.*

[7] C.A. Forbes and J.F. Pierre, The solid fuel-cell future, *IEEE Spectrum, 40-44, October 1993.*

[8] J.M. Fiard and R. Herbin, Numerical Simulation of Solid Oxide Fuel Cells at the Cell and Stack Levels, *Eurogas92, Trondheim, Norway, June 1992.*

[9] J.M. Fiard, R. Herbin, Comparison between finite volume finite element methods for the numerical simulation of an elliptic problem arising in electrochemical engineering, *to appear in Comput. Meth. Appl. Mech. Engin, 115; 315-338, 1994.*

[10] T. Gallouët, An Introduction to Finite Volume Methods, *Cours CEA/EDF/ INRIA, Octobre 1992.*

[11] A.L. Lee, Internal Reforming Development for Solid Oxide Fuel Cells, *DOE/MC/ 22045-2364 report from Institute of Gas Technology, 1987.*

[12] S.V. Patankar, Numerical Heat Transferand Fluid Flow, *Series in Computational Methods in Mechanics and Thermal Sciences, Minkowycz and Sparrow Eds., Mc Graw Hill.*

[13] Ch. Rechenauer and E. Achenbach, Dreidimensionale mathematische Modellierung des stationären und instätionaren Verhaltens oxidkeramischer Hochtemperatur-Brennstoffzellen, *Berichte des Forgschungsxentrums Jülich; 2752.*